



Published in final edited form as:

*Nanoscale*. 2017 June 08; 9(22): 7595–7601. doi:10.1039/c6nr09500c.

## Nanoparticle-induced oxidation of corona proteins initiates an oxidative stress response in cells<sup>†</sup>

Dhanya T. Jayaram<sup>‡,a</sup>, Sabiha Runa<sup>‡,a</sup>, Melissa L. Kemp<sup>b,c</sup>, and Christine K. Payne<sup>a,c</sup>

<sup>a</sup>School of Chemistry and Biochemistry, Georgia Institute of Technology, Atlanta, GA 30332, USA

<sup>b</sup>The Wallace H. Coulter Department of Biomedical Engineering, Georgia Institute of Technology and Emory University, Atlanta, GA 30332, USA

<sup>c</sup>Parker H. Petit Institute for Bioengineering and Biosciences, Georgia Institute of Technology, Atlanta, GA 30332, USA

### Abstract

Titanium dioxide nanoparticles (TiO<sub>2</sub> NPs), used as pigments and photocatalysts, are ubiquitous in our daily lives. Previous work has observed cellular oxidative stress in response to the UV-excitation of photocatalytic TiO<sub>2</sub> NPs. In comparison, most human exposure to TiO<sub>2</sub> NPs takes place in the dark, in the lung following inhalation or in the gut following consumption of TiO<sub>2</sub> NP food pigment. Our spectroscopic characterization shows that both photocatalytic and food grade TiO<sub>2</sub> NPs, in the dark, generate low levels of reactive oxygen species (ROS), specifically hydroxyl radicals and superoxides. These ROS oxidize serum proteins that form a corona of proteins on the NP surface. This protein layer is the interface between the NP and the cell. An oxidized protein corona triggers an oxidative stress response, detected with PCR and western blotting. Surface modification of TiO<sub>2</sub> NPs to increase or decrease surface defects correlates with ROS generation and oxidative stress, suggesting that NP surface defects, likely oxygen vacancies, are the underlying cause of TiO<sub>2</sub> NP-induced oxidative stress.

### 1 Introduction

Titanium dioxide nanoparticles (TiO<sub>2</sub> NPs) are widely used as pigments and photocatalysts in consumer and industrial applications. Previous toxicology studies have shown that these NPs are non-toxic.<sup>1–4</sup> However, our lab<sup>5</sup> and others<sup>6–12</sup> have observed an oxidative stress response to these metal oxide NPs. While currently regarded as safe, long term exposure to even low levels of oxidative stress will ultimately affect human health. We have recently found that incubation of cells (HeLa and BS-C-1) with low, non-cytotoxic concentrations of TiO<sub>2</sub> NPs, in the absence of UV light, produces an oxidative stress response, detected as changes in the expression of the peroxiredoxin family of antioxidant enzymes.<sup>5</sup> Our goal in the research described below was to determine the mechanism of metal oxide NP-induced oxidative stress in the absence of UV light.

<sup>†</sup>Electronic supplementary information (ESI) available. See DOI: 10.1039/c6nr09500c

Correspondence to: Christine K. Payne.

<sup>‡</sup>These authors contributed equally to this work.

TiO<sub>2</sub> NPs are very well studied in terms of ROS generation as it is the ability to generate ROS (*e.g.*, hydroxyl radicals, superoxides, hydrogen peroxide, singlet oxygen), which leads to their use as photocatalysts.<sup>13–15</sup> In comparison, most human exposure to TiO<sub>2</sub> NPs takes place in the dark; for example, in the gut following consumption of food with white pigment TiO<sub>2</sub> NPs or in the lungs following inhalation of TiO<sub>2</sub> NPs in the factories that use them. TiO<sub>2</sub> NPs in sunscreen and cosmetics do not penetrate the skin and include an alumina or silica shell that adsorbs ROS generated by UV exposure.<sup>16</sup> Although less studied than UV-induced ROS, we hypothesized that surface defects, such as oxygen vacancies, could generate ROS, specifically hydroxyl radicals and superoxides.<sup>17–21</sup> Previous work by Colvin *et al.* showed that ROS produced by TiO<sub>2</sub> NPs in the absence of UV light was associated with oxidative stress and cytotoxicity.<sup>10</sup> Additional work has found that TiO<sub>2</sub> NPs in the absence of light produce a classic oxidative stress response in cells including DNA damage, lipid peroxidation, and micronuclei formation.<sup>7</sup> Since most relevant biological exposure takes place in the dark, it is necessary to understand how ROS is generated by metal oxide NPs in the absence of UV light and to determine the link between dark NP-generated ROS and cellular oxidative stress.

In considering the cellular response to NPs, it is important to note that most NPs do not interact directly with cells, but rather through a “corona” of adsorbed proteins on the NP surface.<sup>5,22–28</sup> Both in cell culture and *in vivo*, the major source of extracellular proteins is serum. Previous work in our lab, and others, show that serum proteins used as a nutrient source for cells in culture adsorb onto the surface of TiO<sub>2</sub> NPs forming a protein–TiO<sub>2</sub> NP complex.<sup>5,29,30</sup> The experiments described below were designed to measure ROS production by TiO<sub>2</sub> NPs in the dark and to determine whether the ROS oxidized serum proteins. Experiments used common photocatalytic TiO<sub>2</sub> NPs (analogous to Degussa P25 NPs) and food grade TiO<sub>2</sub> (often referred to by their European Union food additive number, E171). Cellular assays measured oxidative stress in response to these NPs, showing that an oxidized protein corona serves as a cellular signal of oxidative stress. Increasing or decreasing oxygen vacancies through plasma treatment or surface passivation led to increased or decreased oxidative stress, respectively, pointing towards NP surface defects as the origin of ROS-induced oxidative stress in the dark.

## 2 Experimental

### 2.1 Nanoparticles (NPs)

Titanium dioxide nanopowder (21 nm, #718467, equivalent to Degussa P25, Sigma–Aldrich, St Louis, MO), E171 food grade NPs (#13463677, BOC Sciences, Shirley, NY), or carboxylate-modified polystyrene NPs (200 nm, #F8809, Invitrogen/Thermo Fisher, Carlsbad, CA) were used for all experiments. For experiments in 25 cm<sup>2</sup> cell culture flasks (western blots and PCR), TiO<sub>2</sub> NPs were used at a concentration of 400 µg mL<sup>-1</sup>. For experiments in 12-well plates (MTT assays) the concentration of NPs (270 µg mL<sup>-1</sup>) was scaled down based on the number of cells forming a monolayer on the surface of the culture dish to keep the ratio of NPs to cells constant. For experiments with polystyrene NPs, the concentration of NPs (20 pM) was chosen to match the surface area of the TiO<sub>2</sub> NPs used in the corresponding experiment. A TiO<sub>2</sub> NP hydrodynamic diameter of 370 nm (±63 nm, PDI

= 0.36, with a hard corona formed from fetal bovine serum (FBS)), based on dynamic light scattering (DLS), and a polystyrene NP diameter of 200 nm, based on TEM, was used to calculate the surface area.<sup>5</sup> Because the protein corona reduces aggregation of the TiO<sub>2</sub> NPs in solution and provides a better representation of cellular experiments, the hydrodynamic diameter was used for surface area calculations. The diameter of polystyrene NPs is similar as measured by DLS (274 nm ± 11.4 nm, PDI = 0.06) or TEM (200 nm). Since aggregation of polystyrene NPs is minimal, the TEM value was judged to be a better measure of the surface area than the hydrodynamic diameter. All experiments were carried out in the dark.

## 2.2 Surface passivation and plasma treatment

Surface passivation of TiO<sub>2</sub> NPs with a combination of alumina (sodium aluminate, #11138491, Sigma–Aldrich) and silica (#13870285, Sigma–Aldrich) has been described previously.<sup>31</sup> Surface defects were increased using a plasma cleaner (10 min, 18 W, air, Harrick Plasma, Ithaca, NY).

## 2.3 Nanoparticle characterization

Dynamic light scattering (DLS, DynaPro NanoStar, Wyatt Technology, Santa Barbara, CA) was used to measure the hydrodynamic diameter and polydispersity index of the NPs. Zeta potential was measured using a Malvern Zetasizer (Nano-Z, Malvern Instruments, Worcestershire, England). TiO<sub>2</sub> and polystyrene NP concentrations for dynamic light scattering and zeta potential experiments were 400 µg mL<sup>-1</sup> and 8 pM, respectively. Measurements were carried out in triplicate with 3 distinct solutions. Each measurement consisted of 30 runs. Electrophoretic mobility was converted to a zeta potential using the Smoluchowski approximation. TEM (JEOL 100 CX II) of the P25 TiO<sub>2</sub> NPs was carried out previously at the Center for Nanostructure Characterization at Georgia Institute of Technology.<sup>5</sup> X-ray photoelectron spectroscopy (XPS, K-Alpha, Thermo Scientific, Waltham, MA) was used to quantify oxygen vacancies. XPS measurements were carried on 4 distinct samples (2 mg mL<sup>-1</sup>, dried); the representative spectra are shown.

## 2.4 ROS Assays

**2.4.1 H<sub>2</sub>DCF—CM-H<sub>2</sub>DCFDA** (#C6827, Invitrogen/Thermo Fisher) was first deacetylated to produce non-fluorescent H<sub>2</sub>DCF for use in cell-free assays. Specifically, 50 µg of CM-H<sub>2</sub>DCFDA was dissolved in 50 µL of DMSO. 50 µL of methanol was added to the solution followed by 25 µL of 2 M KOH. This solution was vortexed and then incubated at 37 °C for one hour. It was neutralized to pH 7 with HCl prior to use. ROS assays were then carried out according to the manufacturer's instructions. After a 1 h room temperature incubation with H<sub>2</sub>DCF (5 µM in phosphate-buffered saline (PBS)) TiO<sub>2</sub> NPs (400 µg mL<sup>-1</sup>) were removed (8000 rcf, 15 min, ×3) from the solution prior to measurement (Excite: 488 nm; Emit: 523 nm, RF-5301PZ fluorometer, Shimadzu).

**2.4.2 Terephthalic acid (TA)**—Terephthalic acid (2 mM in PBS, #100210, Sigma-Aldrich) was added to an aqueous suspension of TiO<sub>2</sub> NPs (2 mg mL<sup>-1</sup>, 1 h, room temperature). As with the H<sub>2</sub>DCF assay, TiO<sub>2</sub> NPs were removed (8000 rcf, 15 min, ×3) from the solution prior to measurement. The fluorescence intensity of the hydroxyl radical-oxidized product was measured at 434 nm (Excite: 312 nm).

**2.4.3 Nitro blue tetrazolium (NBT)**—NBT (2 mM in water, #298839, Sigma–Aldrich, St Louis, MO) was incubated with TiO<sub>2</sub> NPs (2 mg mL<sup>-1</sup>, 1 h, room temperature), which were removed (8000 rcf, 15 min, ×3) prior to measurement. The superoxide-mediated oxidation of NBT to form insoluble formazan was characterized by a decrease in the NBT absorption at 259 nm (DU 800 spectrophotometer, Beckman Coulter, Brea, CA).

**2.4.4 Amplex Red**—An Amplex Red assay (2 mM in PBS, #A22188, Invitrogen/Thermo Fisher) was carried out according to the manufacturer’s instructions. The generation of H<sub>2</sub>O<sub>2</sub> was detected based on the emission of resorufin at 590 nm.

## 2.5 Measurement of protein oxidation with DNPH

TiO<sub>2</sub> NPs (400 µg mL<sup>-1</sup>) or polystyrene NPs (20 pM) were incubated with 10% FBS (3 mg mL<sup>-1</sup>, 1 mL total volume) in the dark with constant vortexing. After 30 min, the NPs were removed from the mixture by centrifugation (8000 rcf, 15 min, ×3). The protein solution was then incubated with DNPH (10 mM, TCI America, Portland, OR) in 6 M HCl for 15 min, allowing any oxidized proteins to react with the DNPH. To remove unbound DNPH prior to measurement, proteins were precipitated with 50% w/v trichloroacetic acid (Sigma–Aldrich) followed by centrifugation (14 000 rcf, 5 min) and washed in ethanol/ethyl acetate (×3). The pelleted proteins were resuspended in guanidine hydrochloric acid (6 M). The concentration of the bound DNPH (Abs: 370–385 nm) was measured by UV–vis spectroscopy and normalized against the concentration of protein (Abs: 280 nm). Significance was determined by a two-tailed Student’s *t*-test, as noted in the text.

## 2.6 EPR

Aqueous suspensions of TiO<sub>2</sub> NPs (10 mg mL<sup>-1</sup>) and 5,5-dimethyl-1-pyrroline-*N*-oxide (DMPO, 0.02 M, #D5766, Sigma–Aldrich) were drawn into quartz EPR capillaries (#Q-4X. 55, Wilmad-LabGlass, Vineland, NJ) and then inserted into quartz EPR tubes (Wilmad-LabGlass). Spectra were recorded on an EMX EPR 100 X-band spectrometer (Bruker, Billerica, MA).

## 2.7 Cell culture

HeLa cervical carcinoma cells (CCL-2, ATCC, Manassas, VA) were cultured in Minimum Essential Medium (MEM, #61100, Invitrogen) supplemented with 10% FBS (#10437028, Invitrogen) at 37 °C under 5% carbon dioxide. Cells were passaged every 3–4 days.

## 2.8 TiO<sub>2</sub> NP-mediated oxidation of serum proteins

TiO<sub>2</sub> NPs (P25, 400 µg mL<sup>-1</sup>) were incubated with FBS (10%) in MEM, identical to cell culture conditions, for 30 min in the dark with constant rocking. This mixture was centrifuged (8000 rcf, 15 min, ×3) to remove the TiO<sub>2</sub> NPs (Fig. S1A and S1B<sup>†</sup>). We used DNPH to confirm that this 30 min exposure to TiO<sub>2</sub> NPs oxidized the serum proteins. Polystyrene NPs (20 pM) were added to the supernatant of the oxidized proteins allowing a

<sup>†</sup>Electronic supplementary information (ESI) available. See DOI: 10.1039/c6nr09500c

corona to form on the surface of the polystyrene NPs. The protein-polystyrene NP mixture was then transferred to cell culture flasks prior to PCR and western blotting experiments.

## 2.9 Western blots

After treatment with TiO<sub>2</sub> NPs (400 µg mL<sup>-1</sup>, P25, E171, plasma-treated, or passivated) or oxidized corona-PS NPs (20 pM) for 24 hours, cells were lysed with a 1% Triton X-100 lysis buffer with a protease inhibitor (#78441, Halt, Pierce, Rockford, IL) for 30 min at 4 °C. The lysate was separated by centrifugation (14 000 rcf, 20 min, 4 °C). The protein concentration was determined using a BCA assay (#23227, Thermo Fisher). The lysate (20 µg) was diluted 1 : 1 in Laemmli loading buffer (#BP-110R, Boston BioProducts, Ashland, MA) and run on a Tris-glycine SDS gel (#456-1094, Bio-Rad, Hercules, CA) at 230 V for 35 min and then transferred to a PVDF membrane (100 V, 45 min). The membrane was blocked (#MB-070 Rockland Immunochemicals, Pottstown, PA) for 1 h at 4 °C. Primary antibodies were added and incubated overnight at 4 °C in blocking buffer and the membrane was washed with TBS-Tween (3 times, 10 min). Peroxiredoxin 4 (ab59542, Abcam) was diluted 1 : 5000 and actin (#ab3280, Abcam) at 1 : 10 000. Secondary antibodies were incubated for 1 hour at 4 °C in blocking buffer (1 : 10 000, #926-68021 and #926-32212, LI-COR). The membrane was washed twice with TBS-Tween for 10 minutes and then once with TBS. Blots were imaged with an Odyssey Imager (LI-COR) and quantified by densitometry (ImageJ). Significance was determined by a two-tailed Student's *t*-test.

## 2.10 Reverse transcription polymerase chain reaction (RT-PCR)

Polystyrene NPs (20 pM) and oxidized serum proteins (10% FBS oxidized by TiO<sub>2</sub> NPs, as described above) were incubated with HeLa cells (~60% confluent) for 24 h. The cells were then lysed and mRNA was extracted using a RNeasy Mini Kit (#74104, Qiagen, Hilden, Germany) and QIAshredder (#79656, Qiagen). RNA was isolated using the RNase-Free DNase kit (#79254, Qiagen) to remove genomic DNA. Sample volumes were adjusted to ensure that equal amounts of RNA were used for cDNA conversion. Following RNA extraction, cDNA synthesis was performed using an RT<sup>2</sup> First Strand Kit (#330401, Qiagen). Real-time PCR was performed using the RT<sup>2</sup> Profiler PCR Array (Human Oxidative Stress Plus, PAHS-065YC, #330231, Qiagen) in combination with RT<sup>2</sup> SYBR Green ROX qPCR Mastermix (#330522, Qiagen). A StepOnePlus Real-Time PCR System (Applied Biosystems) was used as the real time cyler. The first cycle was 10 min at 95 °C and the 40 subsequent cycles were at 95 °C for 15 seconds and 60 °C for 1 min. Data analysis was performed using the GeneGlobe Data Analysis Center (Qiagen) by selecting a baseline threshold cycle (*C<sub>T</sub>*) of 35 and normalizing against housekeeping genes (beta actin (ACTB), beta-2-macroglobulin (B2M), glyceraldehyde-3-phosphate dehydrogenase (GAPDH), hypoxanthine phosphoribosyltransferase 1 (HPRT1), and large ribosomal protein P0 (RPLP0)). Relative expression levels were calculated using the *C<sub>T</sub>* method ( $2^{-C_T}$ ). Experiments were carried out in triplicate using three distinct cell samples. Significance was determined by a two-tailed Student's *t*-test, as noted in the text.

### 3 Results and discussion

#### 3.1 TiO<sub>2</sub> NPs, in the absence of light, generate ROS

We first probed commonly-used TiO<sub>2</sub> NPs, both industrial P25 NPs (DLS, hydrodynamic diameter = 567 ± 38 nm, PDI = 0.17, ZP = -22 ± 0.5 mV) and food grade E171 NPs (DLS, hydrodynamic diameter = 210 ± 2 nm, PDI = 0.37, ZP = -28 ± 0.5 mV), for possible ROS generation using H<sub>2</sub>DCF (Fig. 1A), a fluorescein derivative that becomes fluorescent upon oxidation by ROS (excitation: 488 nm, emission: 523 nm). Polystyrene NPs, which are not expected to generate ROS, and which did not lead to oxidative stress in previous experiments,<sup>5</sup> were used as a negative control. Hydrogen peroxide was used as a positive control. With any light-based measurement there is the concern that light used for the measurement could excite the TiO<sub>2</sub> NPs or TiO<sub>2</sub> NPs sensitized by a dye or biomolecule. The fluorescent H<sub>2</sub>DCF product is excited at 488 nm. Although this is lower in energy than the 332 nm maximum of these TiO<sub>2</sub> NPs, we were careful to separate the oxidation reaction, carried out in the dark, from the light used for the measurement by removing the TiO<sub>2</sub> NPs (centrifugation at 8000 rcf for 15 min, Fig. S1A and S1B<sup>†</sup>) prior to excitation in the fluorimeter. The H<sub>2</sub>DCF assay demonstrated the production of ROS by TiO<sub>2</sub> NPs, both P25 and E171, in the absence of light.

H<sub>2</sub>DCF is a general probe for ROS that does not discriminate between different species.<sup>32</sup> To distinguish between the specific types of ROS produced, we used probes specific for hydroxyl radicals, superoxides, and hydrogen peroxide. Terephthalic acid (TA) forms a fluorescent product, 2-hydroxyl terephthalic acid (excitation: 312 nm, emission: 434 nm), in the presence of hydroxyl radicals. Experiments show the formation of a fluorescent product following incubation with TiO<sub>2</sub> NPs in the dark (Fig. 1B), demonstrating the TiO<sub>2</sub> NP production of hydroxyl radicals in the absence of UV light. In addition, the use of a hydroxyl radical scavenger, isopropanol, inhibited fluorescence. To confirm that TA is sensitive to only hydroxyl radicals, H<sub>2</sub>O<sub>2</sub> was used as a negative control and Fenton-generated hydroxyl radicals served as a positive control (Fig. S2A<sup>†</sup>). To probe for superoxide we used the reaction between superoxide and nitro blue tetrazolium (NBT, Abs: 259 nm), which leads to the formation of formazan, a water-insoluble product, and a decreased NBT signal.<sup>33</sup> TiO<sub>2</sub> NPs in the dark resulted in decreased NBT absorbance indicating superoxide production, while polystyrene NPs did not lead to a change in signal (Fig. 1C). A superoxide scavenger, superoxide dismutase (SOD), inhibited the reaction of NBT. Control experiments to ensure that NBT was specific to superoxides showed no reaction with H<sub>2</sub>O<sub>2</sub> or Fenton-produced hydroxyl radicals (Fig. S2B<sup>†</sup>). A reaction with xanthine/xanthine oxidase was positive (Fig. S2B<sup>†</sup>). As with the H<sub>2</sub>DCF assay, TiO<sub>2</sub> NPs were removed from the solution prior to TA and NBT measurements. An Amplex Red assay to test for possible H<sub>2</sub>O<sub>2</sub> generation showed no H<sub>2</sub>O<sub>2</sub> (P25 NPs, 2 mg mL<sup>-1</sup>, 1 h, room temperature, data not shown). H<sub>2</sub>O<sub>2</sub> (10 μM) was used as a positive control.

In addition to light-based measurements, hydroxyl radicals and superoxide can also be detected with EPR using DMPO (Fig. 1D), a spin-trapping reagent.<sup>34</sup> DMPO traps hydroxyl radicals to form the DMPO-OH adduct, giving a 4-peak EPR signal. DMPO traps superoxide radicals to form DMPO-OOH, which decomposes to form DMPO-OH. The



EPR spectra of TiO<sub>2</sub> NPs (P25 and E171) showed a characteristic 4-peak signal demonstrating ROS production and trapping by DMPO.

### 3.2 TiO<sub>2</sub> NPs oxidize serum proteins

TiO<sub>2</sub> NPs interact with cells through a layer or “corona” of proteins adsorbed onto the NP surface.<sup>5,29,30</sup> Using proteomics, we previously identified serum proteins adsorbed on the surface of TiO<sub>2</sub> NPs (P25).<sup>5</sup> Complement C3, an immune system protein, was the most abundant protein on the TiO<sub>2</sub> NP surface followed by plasminogen and serum albumin. Based on our observation that TiO<sub>2</sub> NPs produce ROS in the absence of UV light (Fig. 1), we analyzed serum proteins to determine whether this ROS oxidized serum proteins incubated with TiO<sub>2</sub> NPs. As a control, we used polystyrene NPs, which do not produce ROS (Fig. 1A–D).<sup>5</sup>

UV–vis spectroscopy of a carbonyl-reactive probe (2,4-dinitrophenylhydrazine (DNPH)) was used to measure changes in the carbonyl content of serum proteins following incubation with NPs. Radical-induced peptide backbone cleavage leads to an increase in the carbonyl content of proteins.<sup>35</sup> DNPH reacts with carbonyls to form covalently-bound protein-dinitrophenylhydrazone (Abs: 370–385 nm). Protein oxidation is then measured based on the absorption at 375 nm following isolation of the protein from the solution (TCA precipitation and resuspension) to remove the unbound hydrazine.<sup>36</sup> This isolation step also means that the NPs are not present during the measurement and that any oxidation occurred prior to UV–vis spectroscopy. FBS (10%, 3 mg mL<sup>-1</sup>) incubated with TiO<sub>2</sub> NPs (P25 and E171, 30 min, RT) showed an increase in protein oxidation compared to FBS alone or FBS incubated with polystyrene NPs (Fig. 2). In comparison, no change in carbonyl content was observed for serum proteins incubated with polystyrene NPs.

### 3.3 An oxidized protein corona leads to oxidative stress

To determine if the TiO<sub>2</sub> NP-mediated oxidation of proteins leads to oxidative stress, we used TiO<sub>2</sub> NPs (P25) to oxidize serum proteins, removed the TiO<sub>2</sub> NPs by centrifugation (8000 rcf, 15 min, ×3), and then incubated these oxidized proteins with polystyrene NPs to form an oxidized protein corona on non-oxidizing polystyrene NPs. Polystyrene NPs with a non-oxidized protein corona do not lead to oxidative stress.<sup>5</sup> Oxidation of the proteins was confirmed by a DNPH assay, similar to Fig. 2. We then used PCR (Table 1) and Western blotting (Fig. 3) to determine whether these oxidized protein-polystyrene NPs now alter the peroxiredoxins. The same protein bands were observed in the oxidized and unoxidized coronas of the polystyrene NPs (gel electrophoresis, Fig. S3<sup>†</sup>).

We used a PCR array to screen 84 oxidative stress-related genes following the incubation of cells with the oxidized protein-polystyrene NPs (20 pM NPs, 24 h). Changes in gene expression were considered significant for *p*-values < 0.05 for data obtained from 3 distinct experiments. The PCR array showed that 8 genes were altered in comparison with untreated control cells, including three members of the peroxiredoxin family (Table 1). This family of enzymes is responsible for the clearance of peroxides from the cell and is essential to the oxidative stress response.<sup>37–41</sup> Changes in the expression of peroxiredoxin 1, 3, 4, and 5 were also detected in our previous experiments following the incubation of HeLa cells with

TiO<sub>2</sub> NPs (P25) in the presence of serum proteins.<sup>5</sup> The expression of the peroxiredoxins was unaffected by polystyrene NPs in unoxidized cell culture medium.<sup>5</sup> Oxidized proteins in solution, rather than on the surface of NPs, did not alter the expression of any of the peroxiredoxins. The only gene altered by oxidized proteins in solution was heme oxygenase (0.64 ± 0.25-fold change).

Western blotting experiments compared changes in protein expression using an antibody against peroxiredoxin 4. Oxidized serum proteins, incubated with polystyrene NPs, were compared to a control in the absence of NPs with only standard cell culture media (MEM supplemented with 10% FBS) present. The western blot shows a 0.61-fold decrease (±0.04%) in the expression of peroxiredoxin 4 following incubation with the oxidized protein-polystyrene NPs (Fig. 3).

The results described above suggest that a protein(s) oxidized by ROS generated at the surface of TiO<sub>2</sub> NPs then adsorbs onto the surface of a polystyrene NP and that this oxidized protein triggers an oxidative stress response, detected as changes in peroxiredoxin expression. We do not know which specific protein is responsible, and it is likely that a combination of proteins is required since oxidative stress is not observed in response to oxidized proteins in the absence of NPs. Our previous proteomics analysis showed that of the 10 most abundant proteins found on the surface of TiO<sub>2</sub> NPs, 8 of these were also present on the surface of polystyrene NPs.<sup>5</sup>

### 3.4 Oxidative stress correlates with TiO<sub>2</sub> NP surface defects

The decrease in peroxiredoxin 4 observed with PCR (Table 1) and western blotting (Fig. 3) suggests that the protein corona, oxidized by the TiO<sub>2</sub> NPs, signals to the cells that they are under oxidative stress. Underlying this biological response is the question of how TiO<sub>2</sub> NPs generate ROS in the absence of UV light. The characterization of the small amount of ROS generated by TiO<sub>2</sub> NPs in the absence of UV light is rarely studied, as the vast majority of research in this area focuses on the photocatalytic properties of TiO<sub>2</sub>.<sup>13–15</sup> Studies of ROS generation in the dark have been limited to three biological studies,<sup>7,10,21</sup> and our own observations of changes in peroxiredoxins.<sup>5</sup> The most likely source of ROS from TiO<sub>2</sub> NPs in the dark are surface defects, especially oxygen vacancies.<sup>17–21</sup> To test the correlation between surface defects and ROS generation, we used two NP modifications to increase and decrease the surface defects of the TiO<sub>2</sub> NPs, confirmed by X-ray photoelectron spectroscopy (XPS) and EPR (Fig. 4A and B, Table S1<sup>†</sup>), and then measured ROS generation, using H<sub>2</sub>DCF (Fig. 4C), and oxidative stress, using western blotting (Fig. 4D).

Plasma treatment (10 min, 18 W, air, Harrick Plasma Cleaner) was used to increase the surface defects of the TiO<sub>2</sub> NPs (P25).<sup>42–44</sup> XPS shows an increase in the peak at 531 eV associated with oxygen vacancies (Fig. 4A) as well as increased ROS generation (Fig. 4B and C). To examine the effect of decreased surface defects, TiO<sub>2</sub> NPs (P25) were passivated with a silica-aluminum shell on the NP surface,<sup>31</sup> confirmed by XPS (Fig. 4A) and EPR (Fig. 4B). In addition to the XPS scan for oxygen, peaks were also measured for Al 2p and Si 2p (Fig. S4<sup>†</sup>). This surface passivation decreased the amount of ROS generated by the NPs (Fig. 4C). Western blots from three cell samples show that surface passivated TiO<sub>2</sub> NPs (400 µg mL<sup>-1</sup>, 24 h) do not alter peroxiredoxin 4 (Fig. 4D and S5A<sup>†</sup>). In comparison,



plasma-treated and unmodified TiO<sub>2</sub> show a similar decrease in peroxiredoxin 4 (Fig. 4D and S5A<sup>†</sup>), suggesting a threshold response to oxidative stress. An MTT assay of cell health confirmed that the plasma-treated and surface passivated TiO<sub>2</sub> NPs did not decrease cell viability (Fig. S5B<sup>†</sup>).

## 4 Conclusions

Overall, our experiments show that TiO<sub>2</sub> NPs, both industrial P25 and food grade E171 NPs, produce ROS even in the absence of UV light (Fig. 1). This ROS generation, which is correlated with TiO<sub>2</sub> NP surface defects (Fig. 4), oxidizes serum proteins that adsorb onto the surface of the TiO<sub>2</sub> NPs (Fig. 2). These oxidized proteins lead to an oxidative stress response in cells, observed as changes in the peroxiredoxin family of anti-oxidant enzymes (Table 1, Fig. 3 and S6<sup>†</sup> (E171)). While previous work showed that TiO<sub>2</sub> NPs produce low levels of ROS in the dark and that TiO<sub>2</sub> NPs can cause oxidative stress in the dark,<sup>5,7,10</sup> the experiments described above are the first to link the TiO<sub>2</sub> NP-induced oxidation of corona proteins to oxidative stress.

The P25 TiO<sub>2</sub> NPs used in these experiments are the same NPs used in many photocatalytic applications, making them relevant to human health, especially for workers who may inhale them during production.<sup>16,45,46</sup> In addition, people routinely encounter TiO<sub>2</sub> NPs as a white pigment in paint or in food, such as frostings and powders, taking advantage of their high index of refraction for a bright white color. Although both types of NPs are non-toxic, based on conventional toxicology assays,<sup>1–5</sup> it is important to note that long-term exposure to even low levels of oxidative stress can be detrimental to human health. The contemporary theory of the human exposome is based upon small cumulative contributors to disease through lifestyle and environment.<sup>47,48</sup> Our results provide evidence of one such low-level oxidative burden, through TiO<sub>2</sub> NP exposure, that may add to a summative effect on cellular function.

## Supplementary Material

Refer to Web version on PubMed Central for supplementary material.

## Acknowledgments

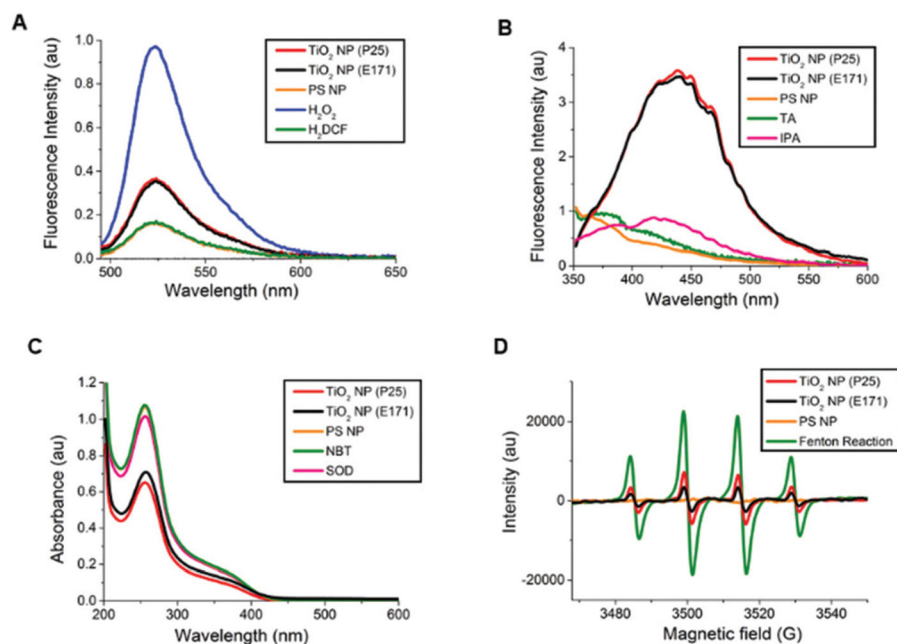
We thank Chrisangela Martin, a member of Project ENGAGES at Georgia Institute of Technology, for assistance with the E171 TiO<sub>2</sub> NP experiments. The authors gratefully acknowledge the HERCULES: Exposome Research Center (NIEHS: P30 ES019776) at the Rollins School of Public Health, Emory University; the Georgia Institute of Technology GT-FIRE program; and a Vasser Woolley Faculty Fellowship to CKP for funding.

## References

1. Boffetta P, Soutar A, Cherrie JW, Granath F, Andersen A, Anttila A, Blettner M, Gaborieau V, Klug SJ, Langard S. Cancer, Causes Control. 2004; 15:697–706. [PubMed: 15280628]
2. Xia T, Kovoichich M, Liang M, Madler L, Gilbert B, Shi HB, Yeh JI, Zink JI, Nel AE. ACS Nano. 2008; 2:2121–2134. [PubMed: 19206459]
3. Llop J, Estrela-Lopis I, Ziolo RF, Gonzalez A, Fleddermann J, Dorn M, Vallejo VG, Simon-Vazquez R, Donath E, Mao ZG, Gao CY, Moya SE. Part Part Syst Charact. 2014; 31:24–35.
4. Xia T, Kovoichich M, Brant J, Hotze M, Sempf J, Oberley T, Sioutas C, Yeh JI, Wiesner MR, Nel AE. Nano Lett. 2006; 6:1794–1807. [PubMed: 16895376]

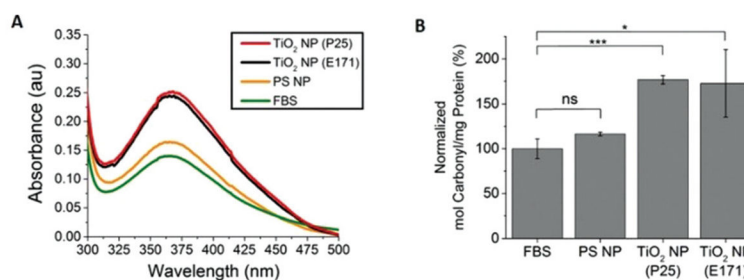
5. Runa S, Khanal D, Kemp ML, Payne CK. *J Phys Chem C*. 2016; 120:20736–20742.
6. De Angelis I, Barone F, Zijno A, Bizzarri L, Russo MT, Pozzi R, Franchini F, Giudetti G, Uboldi C, Ponti J. *Nanotoxicology*. 2013; 7:1361–1372. [PubMed: 23078188]
7. Gurr JR, Wang AS, Chen CH, Jan KY. *Toxicology*. 2005; 213:66–73. [PubMed: 15970370]
8. Jin CY, Zhu BS, Wang XF, Lu QH. *Chem Res Toxicol*. 2008; 21:1871–1877. [PubMed: 18680314]
9. Hussain S, Hess K, Gearhart J, Geiss K, Schlager J. *Toxicol In Vitro*. 2005; 19:975–983. [PubMed: 16125895]
10. Sayes CM, Wahi R, Kurian PA, Liu YP, West JL, Ausman KD, Warheit DB, Colvin VL. *Toxicol Sci*. 2006; 92:174–185. [PubMed: 16613837]
11. Jugan ML, Barillet S, Simon-Deckers A, Herlin-Boime N, Sauvaigo S, Douki T, Carriere M. *Nanotoxicology*. 2012; 6:501–513. [PubMed: 21995316]
12. Kumar A, Khan S, Dhawan A. *J Trans Toxicol*. 2014; 1:28–39.
13. Linsebigler AL, Lu G, Yates JT Jr. *Chem Rev*. 1995; 95:735–758.
14. Fujishima A, Zhang X, Tryk DA. *Surf Sci Rep*. 2008; 63:515–582.
15. Diebold U. *Surf Sci Rep*. 2003; 48:53–229.
16. EPA. *Nanomaterial case studies: Nanoscale titanium dioxide in water treatment and topical sunscreen*. 2010
17. Diebold U, Lehman J, Mahmoud T, Kuhn M, Leonardelli G, Hebenstreit W, Schmid M, Varga P. *Surf Sci*. 1998; 411:137–153.
18. Hugenschmidt MB, Gamble L, Campbell CT. *Surf Sci*. 1994; 302:329–340.
19. Schaub R, Thostrup P, Lopez N, Laegsgaard E, Stensgaard I, Norskov JK, Besenbacher F. *Phys Rev Lett*. 2001; 87:266104. [PubMed: 11800845]
20. Wendt S, Schaub R, Matthiesen J, Vestergaard EK, Wahlstrom E, Rasmussen MD, Thostrup P, Molina LM, Laegsgaard E, Stensgaard I, Hammer B, Besenbacher F. *Surf Sci*. 2005; 598:226–245.
21. Lakshmi Prasanna V, Vijayaraghavan R. *Langmuir*. 2015; 31:9155–9162. [PubMed: 26222950]
22. Doorley GW, Payne CK. *Chem Commun*. 2011; 47:466–468.
23. Doorley GW, Payne CK. *Chem Commun*. 2012; 48:2961–2963.
24. Fleischer CC, Payne CK. *Acc Chem Res*. 2014; 47:2651–2659. [PubMed: 25014679]
25. Walczyk D, Bombelli FB, Monopoli MP, Lynch I, Dawson KA. *J Am Chem Soc*. 2010; 132:5761–5768. [PubMed: 20356039]
26. Lynch I, Cedervall T, Lundqvist M, Cabaleiro-Lago C, Linse S, Dawson KA. *Adv Colloid Interface Sci*. 2007; 7:167–174.
27. Treuel L, Nienhaus GU. *Biophys Rev*. 2012; 4:137–147. [PubMed: 28510093]
28. Park S, Hamad-Schifferli K. *Curr Opin Chem Biol*. 2010; 14:616–622. [PubMed: 20674473]
29. Prasad RY, Wallace K, Daniel KM, Tennant AH, Zucker RM, Strickland J, Dreher K, Kligerman AD, Blackman CF, DeMarini DM. *ACS Nano*. 2013; 7:1929–1942. [PubMed: 23387956]
30. Deng ZJ, Mortimer G, Schiller T, Musumeci A, Martin D, Minchin RF. *Nanotechnology*. 2009; 20:455101. [PubMed: 19822937]
31. Frerichs, S., Morrison, W. US. 20050129634A1. 2005.
32. Kalyanaraman B, Darley-USmar V, Davies KJ, Dennery PA, Forman HJ, Grisham MB, Mann GE, Moore K, Roberts LJ, Ischiropoulos H. *Free Radical Biol Med*. 2012; 52:1–6. [PubMed: 22027063]
33. Goto H, Hanada Y, Ohno T, Matsumura M. *J Catal*. 2004; 225:223–229.
34. Lipovsky A, Tzitrinovich Z, Gedanken A, Lubart R. *Photochem Photobiol*. 2012; 88:14–20. [PubMed: 21988075]
35. Berlett BS, Stadtman ER. *J Biol Chem*. 1997; 272:20313–20316. [PubMed: 9252331]
36. Hawkins CL, Morgan PE, Davies MJ. *Free Radical Biol Med*. 2009; 46:965–988. [PubMed: 19439229]
37. Rabilloud T, Heller M, Gasnier F, Luche S, Rey C, Aebersold R, Benahmed M, Louisot P, Lunardi J. *J Biol Chem*. 2002; 277:19396–19401. [PubMed: 11904290]
38. Finkel T. *J Cell Biol*. 2011; 194:7–15. [PubMed: 21746850]

39. Fujii J, Ikeda Y. *Redox Rep.* 2002; 7:123–130. [PubMed: 12189041]
40. Rhee SG, Chae HZ, Kim K. *Free Radical Biol Med.* 2005; 38:1543–1552. [PubMed: 15917183]
41. Wood ZA, Schroder E, Harris JR, Poole LB. *Trends Biochem Sci.* 2003; 28:32–40. [PubMed: 12517450]
42. Nakamura I, Negishi N, Kutsuna S, Ihara T, Sugihara S, Takeuchi K. *J Mol Catal A: Chem.* 2000; 161:205–212.
43. Ihara T, Miyoshi M, Ando M, Sugihara S, Iriyama Y. *J Mater Sci.* 2001; 36:4201–4207.
44. Jun J, Shin JH, Dhayal M. *Appl Surf Sci.* 2006; 252:3871–3877.
45. Nel A, Xia T, Madler L, Li N. *Science.* 2006; 311:622–627. [PubMed: 16456071]
46. *Current Intelligence Bulletin 63: Occupational Exposure to Titanium Dioxide.* Centers for Disease Control and Prevention and National Institute for Occupational Safety and Health; 2011.
47. Wild CP. *Cancer Epidemiol Biomarkers Prev.* 2005; 14:1847–1850. [PubMed: 16103423]
48. Miller GW, Jones DP. *Toxicol Sci.* 2014; 137:1–2. [PubMed: 24213143]



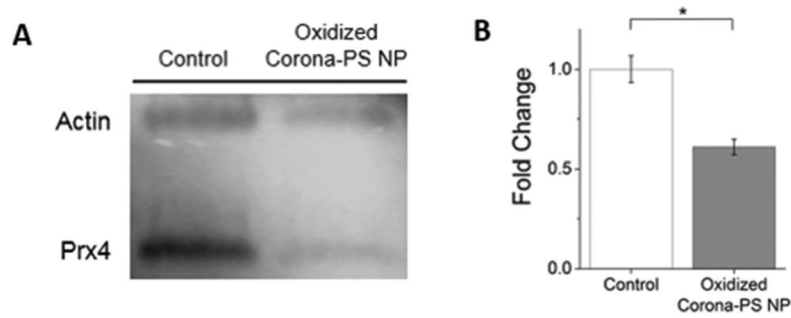
**Fig. 1.**

Generation of ROS by TiO<sub>2</sub> NPs in the dark. (A) Fluorescence spectra of H<sub>2</sub>DCF (5 μM) in response to ROS. TiO<sub>2</sub> NPs (P25 (red) and E171 (black), both 400 μg mL<sup>-1</sup>), were incubated with H<sub>2</sub>DCF in the dark (1 h, RT). Auto-oxidation of H<sub>2</sub>DCF in blank samples (5 μM, green) results in the same signal as polystyrene (PS) NPs (20 pM, matched to the surface area of the TiO<sub>2</sub> NPs, orange). (B) Fluorescence spectra of terephthalic acid (TA, 2 mM) in response to hydroxyl radicals. TiO<sub>2</sub> NPs in the dark (P25 (red) and E171 (black), both 2 mg mL<sup>-1</sup>, 1 h, RT). No emission was observed from TA alone in blank samples (2 mM, green), similar to PS NPs (20 pM, orange). Isopropanol (4% v/v) scavenges the hydroxyl radicals produced by the TiO<sub>2</sub> NPs in the dark (pink). (C) Decreased absorbance of NBT indicates the production of superoxide radicals. TiO<sub>2</sub> NPs (2 mg mL<sup>-1</sup>, 1 h, RT) incubated with NBT in the dark (P25 (red) and E171 (black)). No change was observed from NBT alone in blank samples (2 mM, green) or polystyrene (PS) NPs (20 pM, orange). Superoxide dismutase (SOD, 5mM) scavenges the superoxide produced by the TiO<sub>2</sub> NPs in the dark (pink). (D) EPR spectra of TiO<sub>2</sub> NPs (10 mg mL<sup>-1</sup>, P25 (red) and E171 (black)) and PS NPs (100 pM, orange) with DMPO (0.02 M). Fenton-generated hydroxyl radicals (850 μM, green) were used as a positive control. For all light-based measurements, TiO<sub>2</sub> NPs were removed (8000 rcf for 15 min, ×3) from solution prior to measurement.



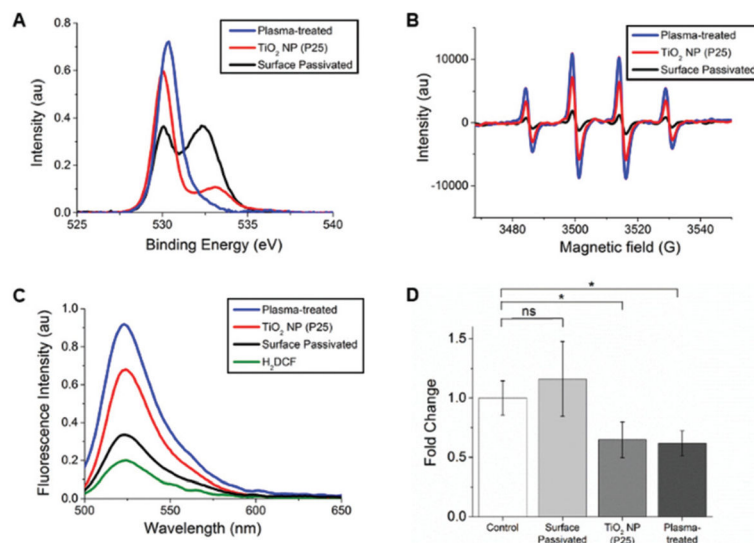
**Fig. 2.**

TiO<sub>2</sub> NP-induced oxidation of serum proteins. (A) Absorption spectra of FBS alone (green) or FBS incubated with TiO<sub>2</sub> NPs (P25 NPs are red, E171 NPs are black) and polystyrene (PS) NPs (orange) in the dark and then tagged with carbonyl-reactive DNPH. (B) The ratio of the 370 nm peak (DNPH) to the 280 nm peak (protein) quantifies the extent of oxidation. Error bars denote  $\pm$  standard deviation for  $n = 3$ . \*\*\* $p < 0.001$ , \* $p < 0.05$ , ns = non-significant. A comparison of the TiO<sub>2</sub> NPs to the PS NPs has the same significance values as the TiO<sub>2</sub> NPs to FBS.



**Fig. 3.** Western blotting of peroxiredoxin 4 following the treatment of HeLa cells with oxidized protein-polystyrene (PS) NPs (24 h, 20 pM). (A) Representative western blot of peroxiredoxin 4 (Prx4). Actin was used as a housekeeping control. Control cells, in the absence of NPs, were incubated with standard cell culture media (MEM + 10% FBS). (B) Densitometric analysis of triplicate samples shows a decrease in peroxiredoxin 4 for oxidized protein-polystyrene (PS) NP-treated cells (24 h, 20 pM, gray) compared to an untreated control (white). Error bars represent  $\pm$  standard deviation, \* $p < 0.05$ .



**Fig. 4.**

Increased or decreased surface defects correlate with ROS generation and oxidative stress. (A) XPS of untreated (red), plasma-treated (blue), and surface passivated (black) TiO<sub>2</sub> NPs was used to monitor changes in oxygen vacancies in response to surface modification. Binding energies and peak areas are listed in Table S1.<sup>†</sup> (B) EPR spectra of control and surface-modified TiO<sub>2</sub> NPs (10 mg mL<sup>-1</sup>) with DMPO (0.02 M). The TiO<sub>2</sub> NP spectrum is replotted from Fig. 1 for comparison. (C) Fluorescence spectra of H<sub>2</sub>DCF (5 μM) in response to ROS. All TiO<sub>2</sub> NPs (400 μg mL<sup>-1</sup>) were incubated with H<sub>2</sub>DCF in the dark (1 h, RT). Auto-oxidation of H<sub>2</sub>DCF (5 μM, green) results in a small positive signal. (D) Western blots were used to quantify changes in cellular oxidative stress as a function of surface modification of TiO<sub>2</sub> NPs. The control shows cells incubated with standard cell culture media (MEM + 10% FBS). Experiments were carried out in triplicate. A representative western blot is shown in Fig. S5A.<sup>†</sup>

**Table 1**

Oxidized corona-polystyrene NP-induced changes in gene expression determined by RT-PCR. Fold changes represent  $2^{-CT}$  ratios between untreated HeLa cells and cells incubated with oxidized protein-polystyrene NPs.  $p < 0.05$  for each gene,  $n = 3$  distinct samples

<b>Gene</b>	<b>Fold change</b>
Antioxidant 1 copper chaperone	3.05 ± 1.08
24-Dehydrocholesterol reductase	6.09 ± 3.06
Glutathione synthetase	2.25 ± 0.48
<b>Peroxiredoxin 3</b>	<b>-4.31 ± 0.16</b>
<b>Peroxiredoxin 4</b>	<b>-2.23 ± 0.20</b>
<b>Peroxiredoxin 5</b>	<b>2.42 ± 0.82</b>
Prion protein	-1.94 ± 0.17
Sequestosome 1	5.10 ± 1.52

Author Manuscript

Author Manuscript

Author Manuscript

Author Manuscript